chemistry proceedings

MDPI

Proceeding Paper

Molecular Docking and Dynamics of a Series of Aza-Heterocyclic Compounds Against PBP2a of Methicillin-Resistant *Staphylococcus aureus* †

Karen Astrid Ortiz-Vargas [1], Rsuini Uri Gutierrez-Aguilar [1], Judit Araceli Avina-Verduzco [1], Hugo Alejandro Garcia-Gutierrez [1], Julio Cesar Ontiveros-Rodriguez [2], Rafael Herrera-Bucio [1,*] and Pedro Navarro-Santos [2,*]

[1] Instituto de Investigaciones Quimico Biologicas, Universidad Michoacana de San Nicolas de Hidalgo, Morelia 58030, Mexico; 1718959h@umich.mx (K.A.O.-V.); rsuini@yahoo.com.mx (R.U.G.-A.); jaavina@umich.mx (J.A.A.-V.); hgarcia@umich.mx (H.A.G.-G.)

[2] CONAHCYT-Instituto de Investigaciones Quimico Biologicas, Universidad Michoacana de San Nicolas de Hidalgo, Morelia 58030, Mexico; julio.ontiveros@umich.mx

* Correspondence: rafael.herrera.bucio@umich.mx (R.H.-B.); pedro.navarro@umich.mx (P.N.-S.); Tel.: +52 443 2239793 (P.N.-S.)

† Presented at the 28th International Electronic Conference on Synthetic Organic Chemistry (ECSOC 2024), 15-30 November 2024; Available online: https://sciforum.net/event/ecsoc-28.

Abstract: *Staphylococcus aureus* is a gram-positive bacterium known to cause mild to severe and potentially fatal infections such as endocarditis, sepsis, meningitis, pneumonia, and bacteremia, among others. The methicillin-resistant strain of *Staphylococcus aureus* (MRSA) arose because the bacterium acquired an additional penicillin-binding protein by lateral gene transfer, known as penicillin-binding protein 2a (PBP2a). It is responsible for cross-linking peptidoglycan chains in the formation of the bacterial cell wall, being a deathly pathogen because it can infect almost sites in the body, so that, the development of novel PBP2a inhibitors and the treatment of infections caused by this bacterium is vital. In this work, a systematic study of molecular docking and molecular dynamics was carried out to determine the stability of a set of ligands type aza-heterocyclic compounds against PBP2a, analyzing their RMSD, H-bonds interactions and binding free energy. In addition, the pharmacokinetic properties are discussed, finding that our proposed ligand **5** is the most promising compound in terms of stability and energetic results.

Keywords: molecular docking; molecular dynamics; penicillin-binding protein 2a; inhibition

Citation: Ortiz-Vargas, K.A.; Gutierrez-Aguilar, R.U.; Avina-Verduzco, J.A.; Garcia-Gutierrez, H.A.; Ontiveros-Rodriguez, J.C.; Herrera-Bucio, R.; Navarro-Santos, P. Molecular Docking and Dynamics of a Series of Aza-Heterocyclic Compounds Against PBP2a of Methicillin-Resistant *Staphylococcus aureus*. *Chem. Proc.* **2024**, *6*, x. https://doi.org/10.3390/xxxxx

Academic Editor(s): Name

Published: 15 November 2024

1. Introduction

The gram-positive bacterium known as *Staphylococcus aureus* was discovered by the physician Alexander Ogston in 1880; it is cocci-shaped, and it belongs to the Bacilli class [1]. In addition, *S. aureus* can cause multiple infections in humans and animals, ranging from uncomplicated infections such as folliculitis or furunculosis to severe illnesses such as endocarditis, septicemia, meningitis, pneumonia, or bacteremia, among others [1]. Methicillin-resistant *Staphylococcus aureus* (MRSA) is acquired by horizontal transfer of the mecA gene, which is responsible for encoding the penicillin-binding protein 2a (PBP2a) that confers resistance [2]. According to the Institute for Health Metrics and Evaluation (IHME) [3], MRSA was the deadliest pathogen and drug combination globally in 2019, with 121,000 deaths attributable to antimicrobial resistance. Overall, the mechanism of action carried out by beta-lactam antibiotics is the irreversible acylation in a functional manner of the enzymes that are responsible for catalyzing the cross-linking steps in the biosynthesis of the peptidoglycan cell wall, i.e., penicillin-binding proteins (PBPs) [4].

However, resistance arises because the formation of the acyl-enzyme intermediate is inefficient, and PBP continues with transpeptidation [2,5].

The PBP2a protein has an active site and an allosteric site, which in several docking and molecular dynamics studies has been observed that when some compound occupies the allosteric site, the active site opens due to conformational changes [6]; nevertheless, there are promising studies of phenolic compounds and flavonoids that can bind to the narrow active site preventing bacterial growth [6,7]. The amino acids that interact within the active site with the compounds are Ser403, Lys 406, Tyr446, Ser462, Asn464, Tyr519, Gln521, Ser598, Gly599, Thr600, Ala601, Glu602 and Met 641 [6,7]. Thanks to the ability of PBP2a to act as a unique transpeptidase during cell wall synthesis against beta-lactam antibiotics, the development of new resistance in PBPs normally produced by *S. aureus* bacteria has been prevented, suggesting a focus on improving binding affinity by increasing non-covalent interactions due to the low acylation efficiency of the protein [5].

2. Methodology

2.1. Pharmacokinetic Analysis

This study was carried out using database searches, docking assessments and molecular dynamics simulations. The proposed ligands [8,9] shown in Figure 1 were consulted in SwissADME [10] in order to obtain certain pharmacokinetic properties.

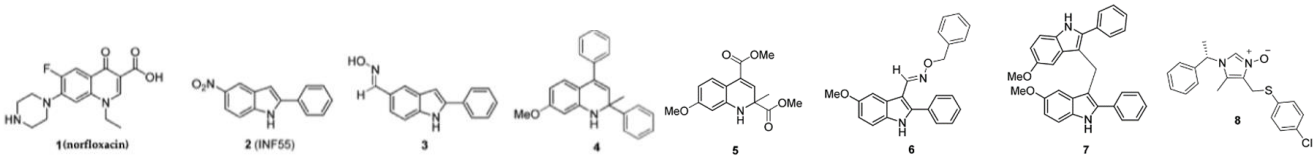

Figure 1. Proposed ligands which are aza-heterocyclic compounds analogous to INF55.

2.2. Molecular Docking

Ligands **1**, **2**, **4**, and **5** in Figure 1 were retrieved from PubChem [11] and ligands **3**, **6**, **7**, and **8** were constructed in the Spartan program [12]; all compounds had their hydrogens added and were prepared in Discovery Studio [13] and AutoDockTools [14]. PBP2a was obtained from the RCSB PDB [15] (PDB ID: 1MWU) with resolution = 2.60 Å co-crystallized with the ligand (2R,4S)-2-[(1R)-1-{[(2,6-dimethoxyphenyl)carbonyl]amino}-2-oxoethyl]-5,5-dimethyl-1,3-thiazolidine-4-carboxylic acid. The receptor was prepared in Chimera [16] and the ligand co-crystallized (**Lig_ref**) was prepared in the same way as the rest of the ligands. Next, the receptor was prepared by adding all the hydrogens, fusing the non-polar ones and adding the Kollman charges using AutoDockTools. Then, AutoDock GR was used to use the **Lig_ref** as a reference along with the receptor, selecting the corresponding flexible amino acids (Ser403, Lys406, Ser462, Asn464 and Ser598) within the grid with a padding of 4.000 Å. Subsequently, AutoDock FR [17] was used to perform the flexible site-specific molecular docking calculations of each of the ligands in the active site, considering a seed number of 1.

2.3. Molecular Dynamics Details

Through Molecular Dynamics simulations, the complexes formed for the most energetically stable conformations of the ligands against the receptor according to the molecular docking assessments were evaluated. Firstly, the ligand parameterization was performed at pH = 7.4 using the "Ligand Reader & Modeler" module of the CHARMM-GUI server [18,19]. After that, the complex was prepared with Chimera and in the "Solution Builder" module of CHARMM-GUI with pH = 7.4, in a rectangular cell of 126 × 126 × 126 $Å^3$, solvated with a TIP3P water model [20] and neutralized by adding NaCl ions at 0.15 M. The force field used for the simulations was CHARMM36m [21] and long-range electrostatic interactions were modeled with the Particle Mesh Ewald (PME) method [22] and

a 12 Å cutoff for non-bonded interactions. Molecular dynamics simulations were carried out using NAMD [23] following the next procedure: Firstly, an energy minimization was performed with a conjugate gradient algorithm [24] for 100,000 iteration steps with a time step of 1.0 fs. Then, the NVT ensemble was used to perform a heating from 0 to 310 K at 1 K intervals for a period of 500 ps, maintaining the 310 K temperature for another period of 500 ps using the Langevin thermostat. Next, an equilibration was performed using the NPT ensemble with conditions of 1 atm and 310 K for a period of 2.5 ns with a time step of 1 fs using the Langevin's thermostat and the Langevin piston Nosé-Hoover barostat [25,26]. Finally, the production stages were carried out with NPT ensemble for a period of 50 ns with a time step of 2 fs.

From the molecular dynamics simulations, the root mean square deviation (RMSD) values of the protein's backbone and of the ligand aligned to the protein were estimated to evaluate the stability of the complexes along the production simulations and the residence of the hydrogen bond interactions were determined. The criterion of the H-bonds determination is considered the maximum donor-acceptor distance of 3.2 Å and a cutoff angle of 50° using the VMD program [27]. For those complexes that showed a higher stability during the simulation, the production simulations were extended to 100 ns calculating the aforementioned properties as well as the binding free energies using the Molecular Mechanics-Generalized Born Surface Area (MM/GBSA) with the tool gmx_MMPBSA [28] for the last 50 ns, exploring an average of 500 snapshots.

3. Results and Discussion

3.1. Pharmacokinetic Results

The pharmacokinetic and physicochemical properties of the proposed ligands are shown in Table 1. It is observed from Table 1 that all ligands have similar physicochemical properties; notwithstanding, **1** and **5** have a Log P coefficient within the value of 1 and have a better solubility in water. Moreover, all the ligands comply with the Lipinski's rules and do not present a false positive alert, according to PAINS.

Table 1. Pharmacokinetic properties of the ligands in Figure 1.

Ligand	Physicochemical Properties				Lipophilicity	Water Solubility		Druglikeness	Medicinal Chemistry
	MW	NRB	HBA	HBD	Log $P_{o/w}$	Log S	Class	Lipinski	PAINS
Lig_ref	382.43	8	7	3	−2.38	−3.25	Soluble	Yes; 0 violation	0 alert
1	319.33	3	5	2	1.04	−3.70	Soluble	Yes; 0 violation	0 alert
2	238.24	2	2	1	1.88	−5.19	Moderately S.	Yes; 0 violation	0 alert
3	236.27	2	2	2	2.24	−5.33	Moderately S.	Yes; 0 violation	0 alert
4	327.42	3	1	1	4.35	−8.54	Poorly S.	Yes; 1 violation	0 alert
5	291.30	5	5	1	1.06	−3.68	Soluble	Yes; 0 violation	0 alert
6	356.42	6	3	1	3.29	−8.64	Poorly S.	Yes; 0 violation	0 alert
7	458.55	6	2	2	4.34	−12.25	Insoluble	Yes; 1 violation	0 alert
8	358.88	5	1	0	4.41	−5.96	Moderately S.	Yes; 1 violation	0 alert

* MW is the molecular weight in gr/mol, NRB is the number of rotable bonds, HBA is the number of H-bond acceptors, HBD is the number of H-bond donors, Log $P_{o/w}$ is the logarithm of the partition coefficient of a solute between *n*-octanol and water calculated with MLOGP, Log S is the logarithm of the water solubility with the method of SILICOS-IT and the class is measured as insoluble < −10 < Poorly < −6 < Moderately < −4 < Soluble < −2 Very < 0 < Highly; The Lipinski's rules indicate what an orally active drug should not have, which are MV ≤ 500, MLOGP ≤ 4.15 N or O ≤ 10 and NH or OH ≤ 5 and Pan-assay interference compounds (PAINS) are chemical compounds that often give false positive results.

3.2. Molecular Docking

The affinity energies obtained from the molecular docking assessments are shown in Table 2. It can be observed from Table 2 that **6** has the best affinity energy followed by **8** and **2**. Whereas, the rest of the ligands have comparable energy with the energy of **Lig_ref**.

All the ligands have a hydrophobic interaction with Tyr446 (For more details: see Figure S1 from Supplementary Materials).

Table 2. Affinity energies (kcal/mol) for the ligands **1–8** against the receptor in molecular docking.

Ligand	Affinity Energies
Lig_ref	−7.6
1	−7.5
2	−8.5
3	−8.4
4	−7.4
5	−8.4
6	−9.5
7	−7.3
8	−8.9

3.3. Molecular Dynamics Results

Figure 2 shows the RMSD values along the 100 ns of simulation for the receptor (Figure 2a) and the ligands aligned to the protein (Figure 2b) respectively. Such complexes corresponded to the most stable and promising complexes obtained from the 50 ns (see Figure S2 and Table S1) in terms of the number of interactions and stability.

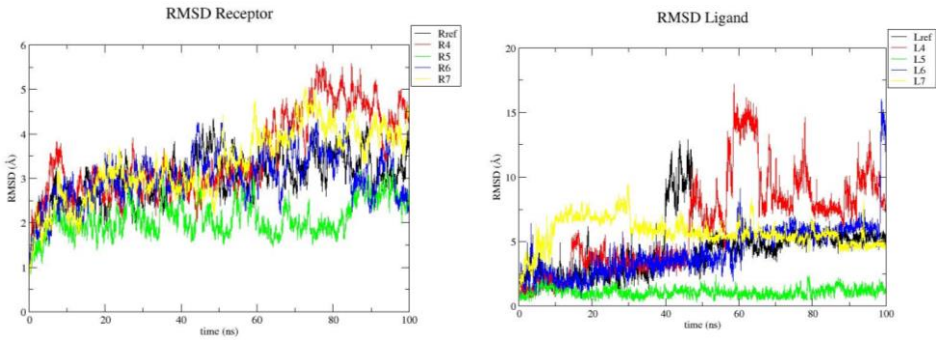

(**a**) (**b**)

Figure 2. RMSD (Å), (**a**) of the receptor and (**b**) of the ligand aligned to the receptor in each complex analyzed for 100 ns.

From Figure 2a, it is observed that the receptor in presence of **5** has less fluctuations followed by the receptor in presence of **Lig_ref**, **6** and **7**, respectively. However, the receptor in presence of **4** has the highest fluctuations. On the other hand, Figure 2b confirms that **5** is the most stabilized ligand. Although **Lig_ref** and **7** were stabilized after 50 ns. Conversely, **6** is observed to be stable during almost the whole trajectory and **4** is destabilized after 45 ns. The maximum and average values of the RMSD are shown in Table S2. Concerning the H-bond interactions, those with a percentage higher than 5% are shown in Table 3.

Table 3. H-bond interactions observed during the 100 ns of simulation.

Ligand	H-bonds Involving the Amino Acids of the Catalytic Site			Other H-Bonds		
	Donator	Acceptor	% of Occupancy	Donator	Acceptor	% of Occupancy
Lig_ref	LIG	GLU602	42.88%	GLN613	LIG	17.56%
	THR600	LIG	9.48%			
	THR600	LIG	5.58%			
	GLU602	LIG	6.18%			
4	TYR446	LIG	27.58%	GLU447	LIG	5.76%

5	ASN464	LIG	65.86%	ALA642	LIG	24.24%
	LIG	THR600	78.04%			
	TYR446	LIG	37.36%			
	ASN464	LIG	5.16%			
6	TYR446	LIG	50.78%	ARG445	LIG	10.70%
	ASN464	LIG	14.44%	THR444	LIG	5.72%
7				GLN613	LIG	5.58%

Table 3 shows that **Lig_ref** and **5** have the highest number of H-bond interactions, where **5** has two interactions greater than 50% with Thr600 and Asn464 respectively; the other ligand that has a higher interaction is **6** with Tyr446; while the rest of the ligands have less interaction. Subsequently, the binding free energy was determined shown in Table 4. From Table 4, it can be observed that **5** is the most stable ligand. Indeed, **5** is more stable **Lig_ref**; in contrast, **6** and **7** have a similar energy but slightly higher than **Lig_ref**, while **4** has the highest energy probably because it did not stabilize during the trajectory.

Table 4. Binding free energies (kcal/mol) obtained from the MMGBSA method of ligand against receptor.

Ligand	Binding Free Energies
Lig_ref	−26.07
4	−10.92
5	−30.05
6	−17.13
7	−18.83

4. Conclusions

On the basis of our chemical-computational study, it was observed that **5**, **6** and **7** have good binding free energies in the calculations performed; however, only **5** is the one that exhibits a value of binding free energy lower than the reference. Regarding the ADMET study, it is observed that all the ligands have ideal pharmacokinetic and physicochemical properties to be good candidates for oral drugs. Therefore, we were able to identify promising compounds for the possible inhibition of the MRSA PBP2a protein, which after several in vivo evaluations, may contribute to the treatment of infections caused by this pathogen.

Supplementary Materials: The following supporting information can be downloaded at: www.mdpi.com/xxx/s1, Figure S1: Interactions and distances (in Å) for ligands **1–8** against the PBP2a receptor; Figure S2: RMSD (Å), (a) of the receptor and b) of the ligand aligned to the receptor in each complex analyzed for 50 ns; Table S1: H-bond interactions for ligands **1–8** during 50 ns of simulation; Table S2: Average and maximum RMSD (Å) (a) of the receptor and (b) of the ligand aligned to the receptor for the 100 ns.

Author Contributions: Conceptualization, software, project administration, writing—review and editing, R.H.-B. and P.N.-S.; methodology, K.A.O.-V., R.H.-B., and P.N.-S.; validation, K.A.O.-V. and R.U.G.-A.; formal analysis, K.A.O.-V. and H.A.G.-G.; investigation, writing—original draft preparation, K.A.O.-V.; resources, P.N.-S.; data curation, K.A.O.-V. and J.A.A.-V.; visualization, K.A.O.-V. and J.C.O.-R.; supervision, R.U.G.-A., J.A.A.-V., H.A.G.-G., J.C.O.-R., R.H.-B. and P.N.-S. All authors have read and agreed to the published version of the manuscript.

Funding:

Institutional Review Board Statement:

Informed Consent Statement:

Data Availability Statement:

Acknowledgments: This work was supported by the Consejo Nacional de Humanidades Ciencias y Tecnologías (CONAHCYT). P. N.-S. Thanks to CONAHCYT for infrastructure grant No. 262232 and K.A. O-V thanks to CONAHCYT for Ms. Sc. scholarship number 1267478.

Conflicts of Interest: The authors declare no conflict of interest.

References

1. Cervantes-García, E.; García-González, R.; Salazar-Schettino, P.M. Características generales del *Staphylococcus aureus*. *Rev. Latinoam. Patol. Clin. Med. Lab.* **2014**, 28–40.
2. Aguayo-Reyes, A.; Quezada-Aguiluz, M.; Mella, S.; Riedel, G.; Opazo-Capurro, A.; Bello-Toledo, H.; Domínguez, M.; González-Rocha, G. Bases moleculares de la resistencia a meticilina en *Staphylococcus aureus*. *Rev. Chil. Infectol.* **2018**, *35*, 7–14.
3. Chan, A. Among Superbugs, MRSA Is at the Forefront of Antimicrobial Resistance. Available online: https://www.healthdata.org/news-events/insights-blog/acting-data/among-superbugs-mrsa-forefront-antimicrobial-resistance (accessed on).
4. Mahasenan, K.V.; Molina, R.; Bouley, R.; Batuecas, M.T.; Fisher, J.F.; Hermoso, J.A.; Chang, M.; Mobashery, S. Conformational Dynamics in Penicillin-Binding Protein 2a of Methicillin-Resistant *Staphylococcus aureus*, Allosteric Communication Network and Enablement of Catalysis. *J. Am. Chem. Soc.* **2017**, *139*, 2102–2110. https://doi.org/10.1021/jacs.6b12565.
5. Lim, D.; Strynadka, N.C.J. Structural basis for the β lactam resistance of PBP2a from methicillin-resistant *Staphylococcus aureus*. *Nat. Struc. Biol.* **2002**, *9*, 870–876. https://doi.org/10.1038/nsb858.
6. Alhadrami, H.A.; Hamed, A.A.; Hassan, H.M.; Belbahri, L.; Rateb, M.E.; Sayed, A.M. Flavonoids as Potential anti-MRSA Agents through Modulation of PBP2a: A Computational and Experimental Study. *Antibiotics* **2020**, *9*, 562.
7. Masumi, M.; Noormohammadi, F.; Kianisaba, F.; Nouri, F.; Taheri, M.; Taherkhani, A. Methicillin-Resistant *Staphylococcus aureus*: Docking-Based Virtual Screening and Molecular Dynamics Simulations to Identify Potential Penicillin-Binding Protein 2a Inhibitors from Natural Flavonoids. *Int. J. Microbiol.* **2022**, *2022*, 9130700. https://doi.org/10.1155/2022/9130700.
8. Gutiérrez, R.U.; Correa, H.C.; Bautista, R.; Vargas, J.L.; Jerezano, A.V.; Delgado, F.; Tamariz, J. Regioselective Synthesis of 1,2-Dihydroquinolines by a Solvent-Free MgBr2-Catalyzed Multicomponent Reaction. *J. Org. Chem.* **2013**, *78*, 9614–9626. https://doi.org/10.1021/jo400973g.
9. Gutiérrez, R.U.; Rebollar, A.; Bautista, R.; Pelayo, V.; Várgas, J.L.; Montenegro, M.M.; Espinoza-Hicks, C.; Ayala, F.; Bernal, P.M.; Carrasco, C.; et al. Functionalized α-oximinoketones as building blocks for the construction of imidazoline-based potential chiral auxiliaries. *Tetrahedron Asymmetry* **2015**, *26*, 230–246. https://doi.org/10.1016/j.tetasy.2015.01.011.
10. Daina, A.; Michielin, O.; Zoete, V. SwissADME: A free web tool to evaluate pharmacokinetics, drug-likeness and medicinal chemistry friendliness of small molecules. *Sci. Rep.* **2017**, *7*, 42717. https://doi.org/10.1038/srep42717.
11. Kim, S.; Chen, J.; Cheng, T.; Gindulyte, A.; He, J.; He, S.; Li, Q.; Shoemaker, B.; Thiessen, P.; Yu, B.; et al. PubChem 2023 update. **2023**, *51*, D1373–D1380. https://doi.org/10.1093/nar/gkac956.
12. Wavefunction_Inc. *Spartan'20 (Version 20.1.3)*; Q-CHEM: 2020.
13. BIOVIA Dassault Systèmes BIOVIA. *Discovery Studio Modeling Environment*; Dassault Systèmes: San Diego, CA, USA, 2019.
14. Morris, G.M.; Huey, R.; Lindstrom, W.; Sanner, M.F.; Belew, R.K.; Goodsell, D.S.; Olson, A.J. Autodock4 and AutoDockTools4: Automated docking with selective receptor flexiblity. *J. Comput. Chem.* **2009**, *16*, 2785–2791. https://doi.org/10.1002/jcc.21256.
15. Berman, H.M.; Westbrook, J.; Feng, Z.; Gilliland, G.; Bhat, T.N.; Weissig, H.; Shindyalov, I.N.; Bourne, P.E. The Protein Data Bank. **2000**, *28*, 235–242. https://doi.org/10.1093/nar/28.1.235.
16. Pettersen, E.F.; Goddard, T.D.; Huang, C.C.; Couch, G.S.; Greenblatt, D.M.; Meng, E.C.; Ferrin, T.E. UCSF Chimera—A visualization system for exploratory research and analysis. *J. Comput. Chem.* **2004**, *25*, 1605–1612. https://doi.org/10.1002/jcc.20084.
17. Ravindranath, P.A.; Forli, S.; Goodsell, D.S.; Olson, A.J.; Sanner, M.F. AutoDockFR: Advances in Protein-Ligand Docking with Explicitly Specified Binding Site Flexibility. *PLoS Comput. Biol.* **2015**, *11*, e1004586. https://doi.org/10.1371/journal.pcbi.1004586.
18. Jo, S.; Kim, T.; Iyer, V.G.; Im, W. CHARMM-GUI: A web-based graphical user interface for CHARMM. *J. Comput. Chem.* **2008**, *29*, 1859–1865.
19. Kim, S.; Lee, J.; Jo, S.; Brooks, C.L., III.; Lee, H.S.; Im, W. CHARMM-GUI ligand reader and modeler for CHARMM force field generation of small molecules. *J. Comput. Chem.* **2017**, *38*, 1879–1886. https://doi.org/10.1002/jcc.24829.
20. Jorgensen, W.L.; Chandrasekhar, J.; Madura, J.D.; Impey, R.W.; Klein, M.L. Comparison of simple potential functions for simulating liquid water. *J. Chem. Phys.* **1983**, *79*, 926–935. https://doi.org/10.1063/1.445869.
21. Huang, J.; Rauscher, S.; Nawrocki, G.; Ran, T.; Feig, M.; de Groot, B.L.; Grubmüller, H.; MacKerell, A.D. CHARMM36m: An improved force field for folded and intrinsically disordered proteins. *Nat. Methods* **2017**, *14*, 71–73. https://doi.org/10.1038/nmeth.4067.
22. Essmann, U.; Perera, L.; Berkowitz, M.L.; Darden, T.; Lee, H.; Pedersen, L.G. A smooth particle mesh Ewald method. *J. Chem. Phys.* **1995**, *103*, 8577–8593. https://doi.org/10.1063/1.470117.
23. Phillips, J.C.; Hardy, D.J.; Maia, J.D.C.; Stone, J.E.; Ribeiro, J.V.; Bernardi, R.C.; Buch, R.; Fiorin, G.; Hénin, J.; Jiang, W.; et al. Scalable molecular dynamics on CPU and GPU architectures with NAMD. *J. Chem. Phys.* **2020**, *153*, 044130. https://doi.org/10.1063/5.0014475.

24. Fletcher, R.; Reeves, C.M. Function minimization by conjugate gradients. *Comput. J.* **1964**, *7*, 149–154. https://doi.org/10.1093/comjnl/7.2.149.
25. Martyna, G.J.; Tobias, D.J.; Klein, M.L. Constant pressure molecular dynamics algorithms. *J. Chem. Phys.* **1994**, *101*, 4177–4189.
26. Feller, S.E.; Zhang, Y.; Pastor, R.W.; Brooks, B.R. Constant pressure molecular dynamics simulation: The Langevin piston method. *J. Chem. Phys.* **1995**, *103*, 4613–4621. https://doi.org/10.1063/1.470648.
27. Humphrey, W.; Dalke, A.; Schulten, K. VMD—Visual Molecular Dynamics. *J. Mol. Graph.* **1996**, *14*, 33–38. https://doi.org/10.1016/0263-7855(96)00018-5.
28. Valdés-Tresanco, M.S.; Valdés-Tresanco, M.E.; Valiente, P.A.; Moreno, E. gmx_MMPBSA: A New Tool to Perform End-State Free Energy Calculations with GROMACS. *J. Chem. Theory Comput.* **2021**, *17*, 6281–6291. https://doi.org/10.1021/acs.jctc.1c00645.